CHAPTER II

FUNDAMENTAL KNOWLEDGE AND LITERATURE REVIEW

2.1 CARBON NANOPARTICLES

Generally, it is known that nanoparticles which could be obtained from arc discharge method are fullerene, carbon nanohorns (CNHs), carbon nanocapsules (CNCs), carbon nanotubes (CNTs) and carbon nanoonions. Among these, carbon nanotubes have gained much more attention due to their prospective characteristics.

2.1.1 C_{60}: Buckminsterfullerene

For several centuries, it was believed that only allotropes of carbon were graphite and diamond. However, in 1985, a new form of carbon, C_{60}: Buckminsterfullerene, was first produced and identified by H. W. Kroto. The structure of C_{60} fullerene is shown in Figure 2.1

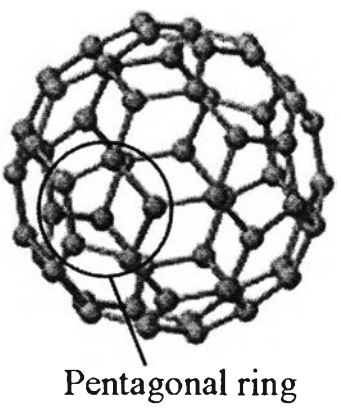

Figure 2.1 C_{60} Buckminsterfullerene

The C_{60} molecule contains 60 atoms arranged in a spherical way, as in a soccer ball (truncated icosahedron). In C_{60}, sp^2 hybridized carbon (as in graphite) is curved by the introduction of pentagonal rings as also shown in Figure 2.1

2.1.2 CARBON NANOTUBE (CNTs)

A carbon nanotube (in appendix A) is a honeycomb lattice rolled into a cylinder as shown in Figure 2.2. The diameter of carbon nanotube is of nanometer size and the length larger than 1 μm. Carbon nanotubes (Iijima *et.al.*, 1991; Dresselhaus *et.al.*, 1996) are specific type of one-dimensional nanomaterial that has sparked people's imaginations. A cover story in American Scientist magazine a few years ago noted that carbon nanotubes could be used to build a space cable connecting the earth and moon. News from NASA indicates that, in the near future, spacecraft may be based solely on carbon material—powered by either fuel cells based on carbon materials or lithium-iron batteries based on nanomaterials. Carbon materials also were featured very prominently in the recent national nanotechnology initiative and were mentioned in the President's State of the Union address, in which he referred to carbon nanotubes as a thousand times stronger than steel.

Carbon certainly is unique in the periodic table; it is truly multifunctional because of its ability to form either $s_p{}^2$ or sp^3 bonds. It can form allotropes with very different structures. For example, diamond with sp^3 bonding has a closely-packed structure, a large elastic modulus, and is electrically insulating. Graphite with sp^2 bonding has a layer structure that is very strong within the layer due to the strong covalent bonds, but weak between the layers due to the weak van der Waals bonds. As a result, graphite can be used as a lubricant and battery electrode because ions can be stored between the graphite layers.

Specially, the electronic structure of a single-wall carbon nanotube is either metallic or semiconducting, depending on its diameter and chirality, and does not require any doping. Thus it can be imagined that the smallest possible semiconductor

devices are likely to be based on carbon nanotubes. Further, the energy gab of semiconducting carbon nanotubes can be varied continuously from 1 eV to 0 eV, by varying the nanotube diameter. Thus, in principle, it may be possible to specify the desired semiconducting properties using only carbon atoms with a specified geometric structure.

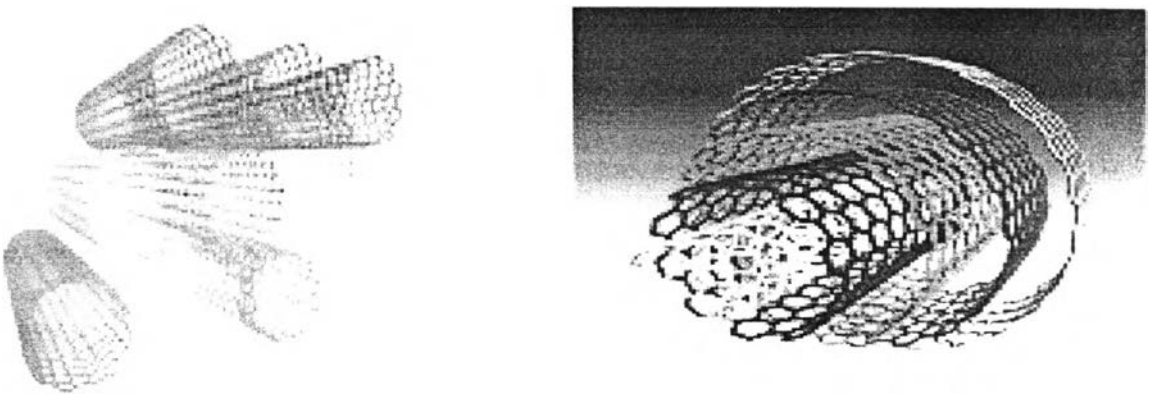

Figure 2.2 (a) The structure of single wall carbon nanotube and
(b) The structure of multi-wall carbon nanotube

2.1.3 CARBON NANOHORN (CNHs) (Iijima *et.al.*, 2004)

Iijima *et.al.*, 2004, the discoverer of carbon nanotubes, now thinks that commercial applications of carbon nanohorns will be realized much earlier than those of carbon nanotubes.

Unlike carbon nanotubes, carbon nanohorns can be made simply without the use of a catalyst. Carbon nanohorn aggregates can be produced with a yield of more than 90% through laser vaporization of carbon at room temperature. These aggregates have a dahlia-like shape with a large number of horn-shaped short single-layered nanotubes that stick out in all directions. The tips of these short nanotubes are capped with five-membered rings. Carbon nanohorns' key characteristic is high adsorbability,

due to their large surface area -- about 400 square meters per gram, but as Prof. Iijima says, "Adsorbed atoms tend to slip easily from the surface of the carbon nanohorns because of their complete graphite surface structure. To hold atoms on the carbon nanohorn surface, either the carbon nanohorns must be modified chemically or their structures must be partially damaged. Various potential characteristics of carbon nanohorns can be displayed by modifying their surface."

The expectation is high for applying carbon nanohorns to fabrication of electrode of fuel cell, among other applications under consideration. Fuel cell electrodes made from carbon nanohorns are expected to help improve the cells' power-generation capacity and extend their lifetime because platinum catalyst nanoparticles disperse among carbon nanohorns and do not aggregate. Carbon nanohorns are also expected as a gas storage material, making by use of their high adsorbability. Carbon nanohorns have for the first time cleared the United States, Department of Energy threshold of commercial reality as methane gas storage material. Carbon nanohorns have also been found to selectively adsorb DNA fractions. Inorganic materials are now used in selecting DNA fractions. However, it is believed that carbon with a high biocompatibility may be a better material than inorganic substances. The Japan Science and Technology Agency (JST) has adopted a project to promote the application of carbon nanohorns in the biotechnology field as one of its "Solution Oriented Research and Technology" projects. This project started in January 2003 for a better understanding of the adsorption to carbon nanohorns, as well as for studying surface modification methods for controlling their selective adsorbability. Carbon nanohorns are shown in Figure 2.3.

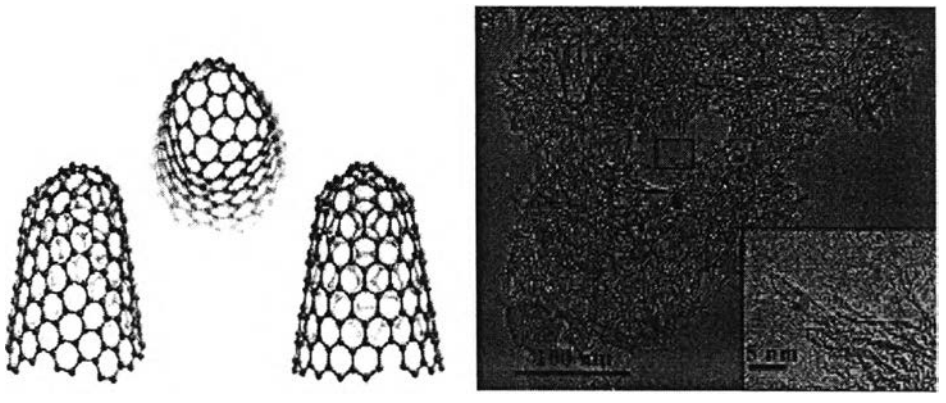

Figure 2.3 Carbon nanohorns (CNHs) model

and TEM image of CNHs [10]

2.1.4 CARBON NANOCAPSULE AND MULTI-SHELLED CARBON NANOPARTICLES (CHCs)

It has been suggested that carbon-coated magnetic nanoparticles might have important applications in many areas such as magnetic data storage, xerography and magnetic resonance imaging. A typical example of carbon nanocapsule is shown in Figure 2.4. It is a particle containing encapsulated by graphene layers. The role of the carbon layer would be to isolate the particles magnetically from each other, thus avoiding the problems caused by interactions between closely spaced magnetic bits, and to provide oxidation resistance. In addition, the lubricating properties of the graphitic coatings might be helpful in magnetic recording and applications. The potential of important applications has motivated a significant amount of research on the encapsulation of magnetic materials in carbon nanoparticles.

Carbon nanocapsules which there are no metal as core particle can be called as multi-shelled nanoparticles. These particles consist several of graphene sheets in various shapes such as spherical, polyhedral, or short-tube.

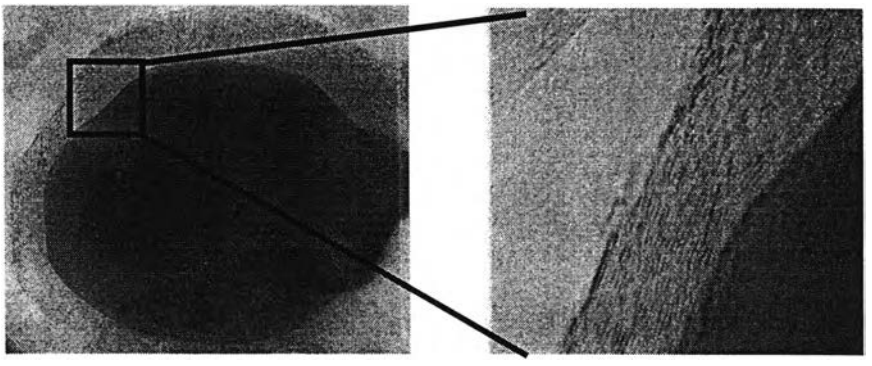

Figure 2.4 TEM image of carbon nanocapsule show low and high magnification, respectively

2.1.5 CARBON NANO ONION

Carbon nano onion have a central shell about 0.7-1 nm in diameter, i.e. very close to the diameter of C_{60}. The onions are almost always quasi-spherical in shape, as shown in Figure 2.5. The detailed atomic structure of carbon onions has been the subject of much discussion. Some authors have assumed that the particles consist of nested fullerenes, as suggested by Kroto in the article which accompanied Ugarte's paper . A plausible model for onion structure is one made up of concentric 'magic number' (or Goldberg Type I) fullerenes. These fullerenes have N carbon atoms, where $N = 60b^2$, so that the first five are C_{60}, C_{240}, C_{960} and C_{1500} (with all fullerenes having the Ih symmetry). In an onion constructed from these fullerenes, the spacing between successive shells would be ~0.34 nm, i.e. close to the interlayer spacing in graphite, and to the spacing observed experimentally for onions. A possible problem with this model is that most theoretical studies suggest that large fullerenes (C_{240} and larger) should be faceted, rather than spheroidal. Although this faceting is only evident in certain directions, as shown in Figure 2.5 ,one would expect some of the onions in experimental images to appear quite strongly faceted, rather than spheroidal. However, work by a Japanese group led by K. Takayanagi has suggested that the

onions become preferentially aligned with C_5 axis parallel to the beam, as a result of interaction with the magnetic field of the lenses, thus explaining their almost circular profiles. Detailed analysis of high resolution images by Zwanger and Banhart has also provided support for the Goldberg-fullerene model.

Other workers have attempted to account for the sphericity of carbon onions by putting forward alternative structures. These have generally involved the introduction of heptagonal rings as well as pentagons into the structure of the carbon shells. The resulting structures are much more spherical than the corresponding fullerenes, as can be seen in Figure2.6 This shows a shell containing 1500 carbon atom which contains 132 pentagons and 120 heptagons, taken from the work of Humberto and Mauricio Terrones. Buckyballs can be thought of as zero-dimensional structures. They are a truly nanoscale material, because the diameter of the molecule is about 1 nm (10^{-9}m). Assembled into a solid with weak intermolecular bonding, buckyballs have very interesting properties. For example, if C_{60} molecules are charged, the sphericity of this structure suggests that it may represent a more realistic model for the outer shells of carbon onions than the 'perfect fullerene' model.

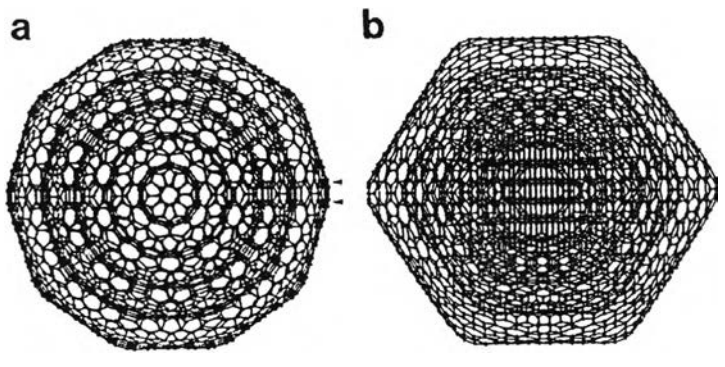

Figure 2.5 Two views of a five-shell carbon onion with the 'concentric fullerene' structure, along (a) C5 and (b) C2 symmetry axes [6]

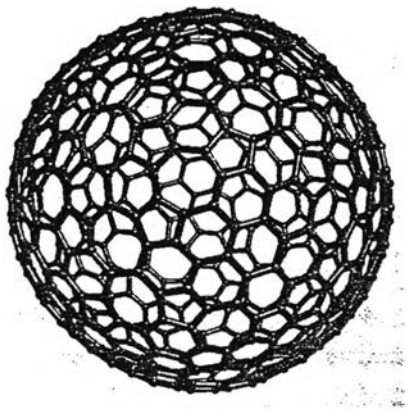

Figure 2.6 The Terrones model of carbon onion structure, incorporating pentagon-heptagon patches [6]

2.2. Mechanism of carbon nanoparticles formation in an arc discharged submerged in water (Sano *et.al.*, 2004)

Sano *et. al.*, 2004 have succeeded in fabrication carbon nanoparticles by using arc discharge submerged in distilled water. They have also proposed an informative explanation on the formation of those carbon nanoparticles. The mechanism proposed could be summarized as follows,

2.2.1 GAS BUBBLE FORMATION

Two types of structures, carbon onions and elongated structures such as carbon nanotubes, were obtained in the water arc. N. Sano proposes an initial model to explain the production mechanism of the two types of structures. Figure 2.7 describes the model of the reaction zone. There is a plasma zone between electrodes surrounded by a gas bubble due to vaporization of the surrounding liquid as the arc temperature is estimated to be around 4000 K (the sublimation temperature of carbon). In fact, this gas bubble can be regarded as a microwater-cooling reaction

chamber that enables rapid quenching of the arc discharge. The main gas components are CO and H_2 produced by the reaction of C atomic vapor and H_2O at the gas-liquid interface as

$$C + H_2O \rightarrow CO + H_2. \qquad (1)$$

To produce CO at the gas-liquid interface, C atomic vapor must be present at this interface. It is therefore reasonable to expect that C atomic vapor exists wholly in the bubble surrounding the discharge.

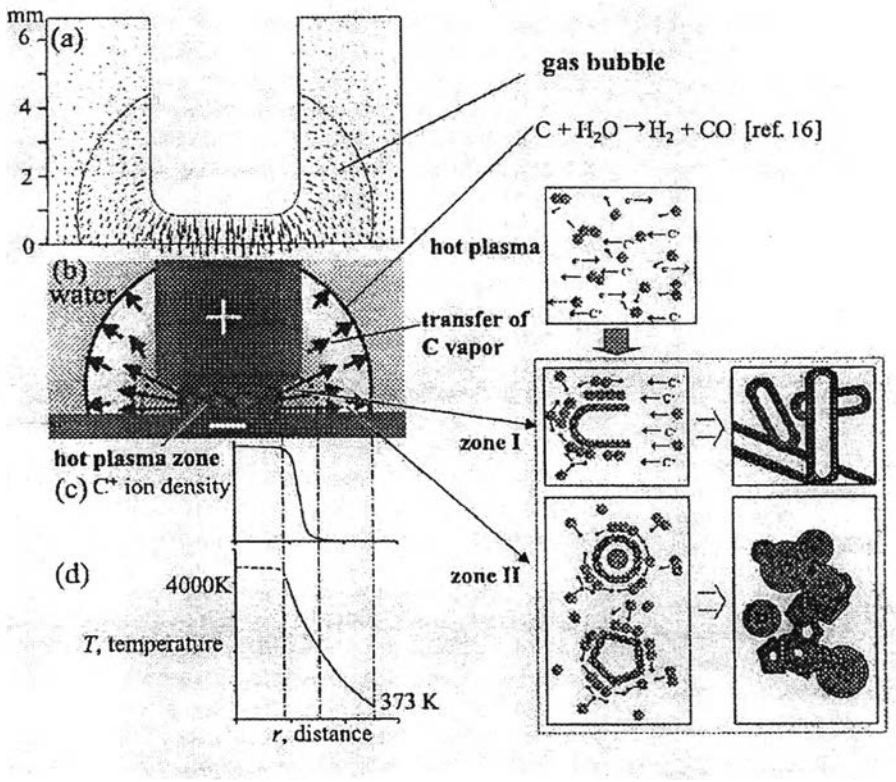

Figure 2.7 Formation mechanism of nanoparticles in a water arc. (Sano *et al.*, 2002)

Carbon is vaporized by the hot arc plasma at the graphite anode, and the carbon vapor can be converted into nano-structural products. The liquid plays roles to

provide the gas components into the plasma reaction zone and to realize rapid quenching of the carbon vapor. In the region with high current density, the products with long structure such as nanotubes should be preferably produced by directional growth. Whereas, in the low current density region outside the high discharge current region, the relatively isotropic structures such as shelled particles may be preferably produced. The structures and some physical properties of the products can be controlled by varying some operational parameters as mentioned above.

(a) Relative electric field strength, shown by arrows, between a rod anode and a flat cathode in a gas bubble surrounded by water

(b) Direction of thermal expansion from plasma to the water interface

(c) Qualtitative ion density distribution.

(d) Temperature gradient obtained from eq. (2) assuming q_c, Q_R, and dT/dt = 0. The formation of elongated nanoparticles in zone (I) and onions in zone (II) is also shown schematically.

2.2.2 NANOPARTICLE FORMATION

The extremely sharp temperature gradient in this gas bubble from the hot plasma region to the gas-water interface is essential to cause rapid solidification of the vaporized carbon. The temperature at the hot plasma is estimated to be approximately 4000 K (The melting and boiling points of graphite are 3823 and 4203 K, respectively), while the temperature at the gas-water interface is the boiling point of water, 373 K.

To estimate the approximate temperature gradient, it can be simply assumed that the heat transfer occurs in a radial direction from the center of the plasma. Then the equation of heat balance can be expressed as

$$-\frac{d}{dr}\left(4\pi r^2 q_k\right)-\frac{d}{dr}\left(4\pi r^2 q_c\right)+4\pi r^2 Q_R = 4\pi r^2 \rho C_p \frac{dT}{dt}, \qquad (2)$$

where r, q_r, q_c, Q_R, C_p, T, and t are the distance from the arc center, heat transfer rate by thermal conductivity, heat transfer rate by convection, reaction heat, density of gas, specific heat of gas, temperature, and time, respectively. To simplify the calculation, q_c, Q_R, and dT/dt are assumed to be zero. If q_k is expressed by Fourier's law of thermal conductivity with a proportional constant k as q_k = -kdT/dr with boundary conditions, T = 4000 K at r = 2 mm and T = 373 K at r = 5 mm, the average temperature gradient in the gas bubble is estimated to be 1209 K/mm. It is noted that this simple calculation is only to give a rough approximation of the temperature gradient.

In fact, q_c, Q_R, and dT/dt should be significant in the real system and all parameters must be highly space and time dependent. Also, the expansion rate of C vapor from the hot plasma zone to cold region can be estimated by a simple approximation. If all the graphite consumed in the anode is assumed to be converted to C vapor, the volumetric C vapor expansion rate is calculated to be 5.30×10^{-5} m^3/s at 4000 K if ideal gas conditions with 1 atm pressure are assumed. If the hot plasma zone between electrodes with a 1 mm gap is assumed as a cylindrical zone with a 2 mm diameter, the expansion velocity can be obtained by dividing this volumetric expansion rate by the surface area of this assumed hot plasma zone, resulting in a velocity of 4.2 m/s. This high expansion velocity enables C vapor to transfer into the cold zone of the bubble readily. The cold zone can be categorized into two parts: (I) that where the quenching of C vapor occurs within the ion current adjacent to the hot plasma zone and (II) that without the ion current outside zone (I).

Although it had not been obtained the distribution of the ion current density in the system at present, and it can be provided a map of simulated electric field in a configuration that is close to our electrode shapes in Figure 2.7. This simulation does not include the effect of the C vapor expansion. In zone (I), elongated structures such as nanotubes are expected to be produced because of their epitaxial growth in the C ion current. On the other hand, in zone II, three-dimensional (3D) isotropic growth of nanoparticles is preferable because of the absence of an axis of symmetry. In this case, onions may be produced.

2.2.3 FLOATATION OF CARBON NANOPARTICLES

Subsequent to the formation of onions, they cluster into larger van der Waals crystals. N. Sano et al., 2002 find that these clusters readily float to the top of the water surface and these floating powder remains separates at the surface of the water even after vigorous dispersion through ultrasonication. In order to investigate the mechanisms responsible for floatation of the onion powder by calculate the true density. It resulted in a mean density of particles of 1.64 g/cm^3. It is noteworthy that it is higher than water although it is lower than graphite 2.25 g/cm^3. The density is comparable to that of well known caged nanoparticles such as C_{60} and nanotubes whose densities are 1.72 and 1.2-2.0 g/cm^3 respectively. Hence, floatation of the particles cannot be ascribed to their weight but more likely to their hydrophobic surface. In fact, the particles can be dispersed well in organic solvents such as acetone, toluene and n-hexane. In their arc-in-water system, onions are naturally agglomerated and float, being separated from the other large products that settle to the bottom of the beaker.

2.3 Polymer nanocomposite (Nanocomposite Science and Technology. Edited by P.M. Ajayan *et.al.*, 2003)

Polymer composites are important commercial materials with applications that include filled elastomers for damping, electrical insulators, thermal conductors, and high-performance composites for use in aircraft. Materials with synergistic properties are chosen to create composites with tailored properties; for example, high-modulus but brittle carbon fibers are added to low-modulus polymers to create a stiff, lightweight composite with some degree of toughness. In recent years, however, we have reached the limits of optimizing composite properties of traditional micrometer-scale composite fillers, because the properties achieved usually involve compromises. Stiffness is traded for toughness, or toughness is obtained at the cost of optical clarity. In addition, macroscopic defects due to regions of high or low volume fraction of filler often lead to breakdown or failure. Recently, a large window of opportunity has opened to overcome the limitations of traditional micrometer-scale polymer composites – nanoscale filled polymer composites – in which the filler is <100 nm in at least one dimension (Figure 2.8).

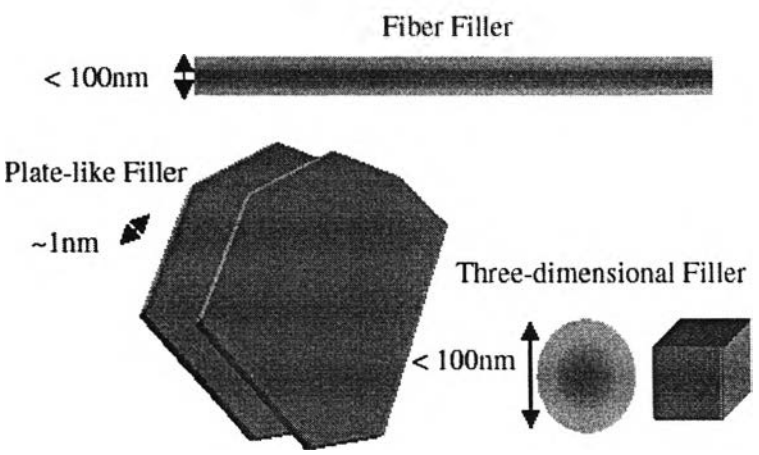

Figure 2.8 Schematic of nanoscale fillers

Although some nanofilled composites (carbon black and fumed silica filled polymers) have been used for more than a century, research and development of nanofilled polymers has greatly increased in recent years, for several reasons. First, unprecedented combinations of properties have been observed in some polymer nanocomposites. For example, the inclusion of equi-axed nanoparticles in thermoplastics, and particularly in semi crystalline thermoplastics, increases the yield stress, the tensile strength, and Young's modulus compared to pure polymer. A reason for the large increase in research and development efforts was the 'discovery' of carbon nanotubes in the early 1990s. Although more careful review has shown that nanotubes have been observed since the 1960s, it was only in the mid-1990s that they were made in the quantities required for property evaluation of composites. The properties of these carbon nanotubes, particularly strength and electrical properties are significantly different from those of graphite and offer exciting possibilities for new composite materials.

2.3.1 Nanoscale fillers

Nanoscale fillers come in many shapes and sizes. For ease of discussion, we have grouped nanofillers into three categories (Figure 2.8). Fiber or tube fillers have a diameter <100 nm and an aspect ratio of at least 100. The aspect ratios can be as high as 106 (carbon nanotubes). Plate-like nanofillers (Figure 2.8) are layered materials typically with a thickness on the order of 1 nm, but with an aspect ratio in the other two dimensions of at least 25. Three dimensional (3D) nanofillers are relatively equi-axed particles <100 nm in their largest dimension. This is a convenient way to discuss polymer nanocomposites, because the processing methods used and the properties

achieved depend strongly on the geometry of the fillers. Such as nanofiber or Carbon nanotubes Fillers:

Micrometer-size carbon tubes, which are similar in structure (but not in dimensions) to the recently discovered multi-walled carbon nanotubes, were first found in 1960 by Roger Bacon. These nanosized, near-perfect whiskers (termed nanotubes) were first noticed and fully characterized in 1991 by Sumio Iijima of NEC Corporation in Japan. He was investigating the surface of carbon electrodes used in an electric arcdischarge apparatus that had been used to make fullerenes. Several exciting developments have taken place in this field since then, and several books document recent progress.

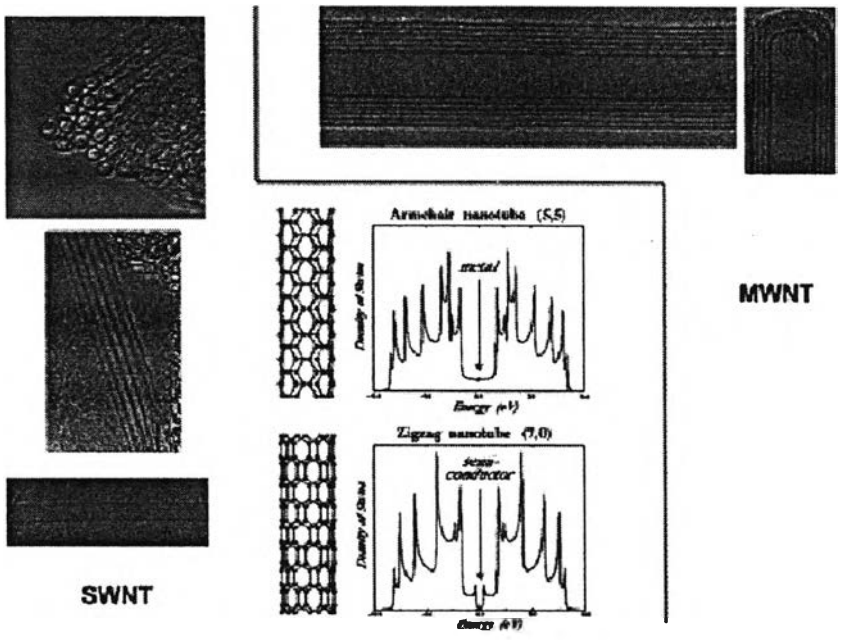

Figure 2.9 HRTEM image showing the SWNT in bundles, (b) HRTEM images of a MWNTalong its length and at the end, (c) schematic showing two examples of the helicity that occurs, zigzag and armchair

The first nanotubes observed were multi-walled nanotubes (MWNT). MWNTs consist of two or more concentric cylindrical shells of graphene sheets coaxially arranged around a central hollow core with interlayer separation as in graphite (0.34

nm). In contrast, single-shell or sir ;le-walled nanotubes (SWNT) are made of single graphene (one layer of graphite) cylinders and have a very narrow size distribution (1–2 nm). Often many (tens) single-shell nanotubes pack into larger ropes. Figure 9 shows electron micrographs of SWNT and MWNT. Both types of nanotubes have the physical characteristics of solids and are microcrystals, although their diameters are close to molecular dimensions. In nanotubes, the hexagonal symmetry of the carbon atoms in planar graphene sheets is distorted, because the lattice is curved and must match along the edges (with dangling bonds) to make perfect cylinders. This leads to a helical arrangement of carbon atoms in the nanotube shells. Depending on the helicity and dimensions of the tubes, the electronic structure changes considerably. Hence, although graphite is a semi-metal, carbon nanotubes can be either metallic or semiconducting. Nanotubes are closed by fullerene-like end caps that contain topological defects (pentagons in a hexagonal lattice). The electronic character of the ends of these tubes differs from the cylindrical parts of the tubes and is more metallic, due to the presence of defects in these regions. The discovery of nanotubes has complemented the excitement and activities associated with fullerenes. Although fullerenes have fascinating physical properties, their relevance in the nanocomposite field is limited, so we shall restrict our discussion of carbon nanostructures to nanotubes.

2.3.2 Processing of Polymer Nanocomposites

One of the key limitations in the commercialization of nanocomposites is processing. Early attempts at clay-filled polymers required processing that was not commercially feasible, but this situation has changed. Similarly, processing of other nanocomposites is becoming easier and more commercially viable as our

understanding improves. A primary difficulty is proper dispersion of the fillers. Without proper dispersion and distribution of the fillers, the high surface area is compromised and the aggregates can act as defects, which limit properties. To facilitate discussion, we will define the state of aggregation in those nanocomposites. Distribution of a nanofiller describes the homogeneity throughout the sample, and the dispersion describes the level of agglomeration. Figure 2.10 schematically illustrates good distribution but poor dispersion (a), poor distribution and poor dispersion (b), poor distribution but good dispersion (c), and good distribution and good dispersion (d). The state of aggregation is further defined in layered silicate/polymer nanocomposites later in this chapter.

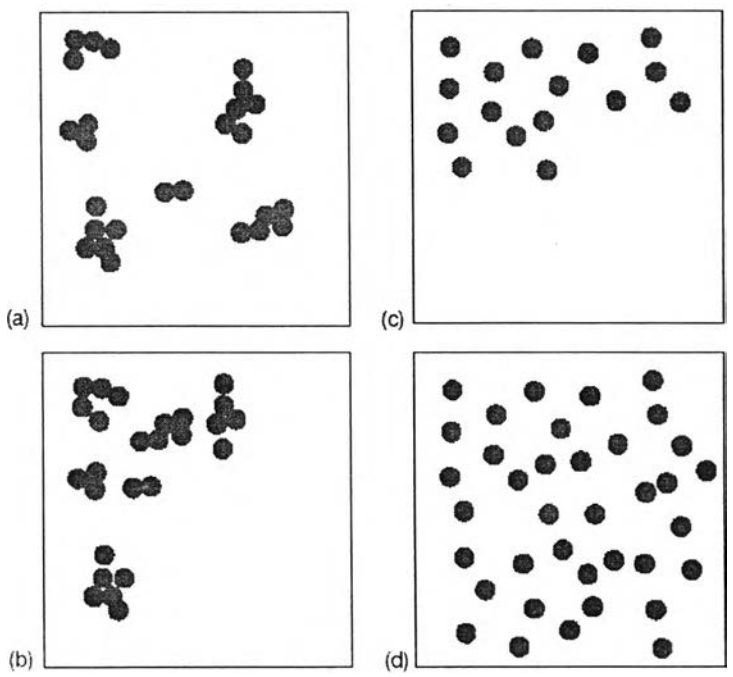

Figure 2.10 A schematic illustrating the difference between dispersion and distribution and giving examples of good and poor for each.

2.3.2.1 Nanotube/Polymer Composites

The processing of nanotube/polymer composites is still in its infancy. Although nanotubes have been incorporated into composites commercially, the literature describing the processes is limited. Significant issues remain to be solved

about purification, dispersion, and bulk processing. The ability to disperse SWNT and MWNT into a polymer may be the most critical processing parameter for controlling properties. Nanotubes that are in clumps or are agglomerated with other carbonaceous materials create defect sites that will initiate failure. In addition, they limit the efficiency with which the nanotubes carry load. This limitation has been illustrated explicitly in both polymer and ceramic matrix composites. CVD-grown MWNT, which are easily dispersed and less agglomerated, increased the modulus and strength of polystyrene without compromising the strain-to-failure factor significantly. Other work on arc-discharge-grown MWNT, which were not fully purified and not as well dispersed, did not show the increase in toughness observed for well-dispersed MWNT. Similarly, the toughness of MWNT/alumina composites with excellent dispersion increased significantly compared to composites with somewhat worse dispersion. Dispersion has been achieved primarily by sonication of nanotubes in a solvent. The most focused efforts have been on the dispersion of SWNT. Chemical modification of the surface with the aid of surfactants, by functionalization of the end-caps with long aliphatic amines, or by functionalization of the sidewalls with fluorine or alkanes has resulted in stable suspensions of nanotubes. None of these methods is ideal for composite processing. The use of surfactant results in an impurity in the composite. Functionalizing the ends limits further chemical modifications for controlling bonding with the matrix, and modification of the sidewalls can affect the mechanical properties. As an alternative, the best solvents for direct dispersion of SWNT were identified as NMP, DMF, hexamethylphosphoramide, cyclopentane, tetramethylene sulfoxide, and e-caprolactone. These solvents are all strong Lewis bases without hydrogen donors, although not all solvents with these characteristics were good solvents for SWNT. After dispersion, drying the dispersion on a glass slide

and placing resin directly onto a thin film of nanotubes can produce small-scale composites.

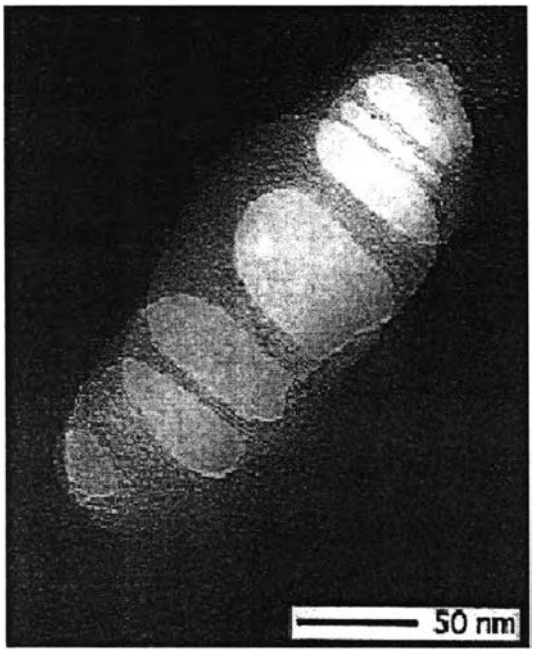

Figure 2.11 Transmission electron micrograph of aligned singlewall carbon nanotube ropes bridging an elliptical hole in a polymer film.

Mixing both the nanotubes and the polymer in the presence of a solvent, often with the help of a surfactant, can also produce composites. Figure 2.11 shows the wetting and the dispersion of SWNT dispersed in ethanol and then mixed with an epoxy resin. Figure 2.12 shows the dispersion achieved with CVDgrown MWNT, dispersed in toluene with dissolved polystyrene and casting films. Excellent dispersion was achieved. Nanotubes have also been dispersed directly into liquid urethane acrylate polymer, methylmethacrylate monomer, and epoxy resin, followed by curing or polymerization. Damage to the nanotubes is a tradeoff that must be considered.

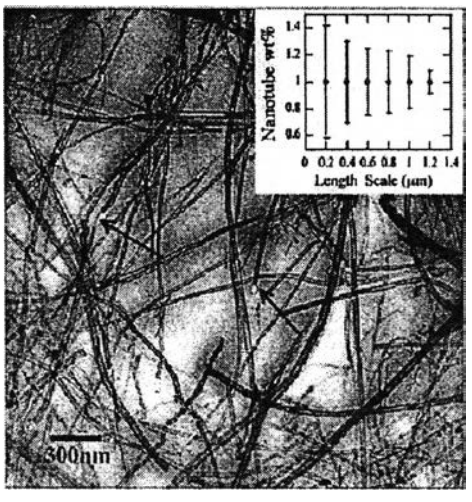

Figure 2.12 Transmission electron micrograph of MWNT-PS film in which the nanotubes are homogeneously distributed in the polystyrene matrix at a 1 lm length scale.

Nanofibers have been successfully melt-mixed with polyphenylene ether/polyamide matrices in a twin screw extruder. This process has led to a commercial product in conductive thermoplastics for electrostatic painting without the loss of mechanical properties. An interesting composite processed from nanotubes is a macroscopic fiber that is a mixture of nanotubes and a traditional material used for carbon fibers, such as pitch or PAN. This was achieved with a pitch-based matrix and led to interesting improvements in properties, because the pitch fibers were not subjected to the typical high temperature processing.

2.3.2.2 Polypropylene and Polyethylene Matrices

Nonpolar polymers are very difficult to intercalate into smectic clays, because the clays are strongly polar. This challenge has been met by first intercalating stearylamine into montmorillonite and synthetic mica. Melt-mixing the organoclays with maleic anhydride-modified polypropylene oligomers results in PP-MA intercalation. The modified organoclay is then melt-mixed with a polypropylene

matrix. There is a balance between creating a polar oligomer with enough maleic anhydride to intercalate well, but nonpolar enough to mix with the polypropylene. Unfortunately, the oligomer limits the extent of property improvement achieved to date. Polyethylene has also been successfully melt-mixed with modified montmorillonite and saponite after ion exchange with dioctadecyldimethylammonium bromide. The degree of dispersion is not excellent, and the layers are certainly not exfoliated; yet, significant modification of both the crystal structure and properties has been observed.

2.3.2.3 Polymethylmethacrylate/Polystyrene Matrices

The processing of clay/PMMA or clay/PS composites was first done by directly intercalating the monomer into the clay, followed by polymerization. This method was not successful in exfoliating the clays. At issue again is the compatibility between the clay and the monomer. One solution for PMMA has been to use appropriate ammonium salts, which may be reactive. Another solution is to use a comonomer as a compatibilizer. A similar solution was found for polystyrene by using the reactive cationic surfactant vinylbenzyldimethyldodecylammonium as the intercalant. Exfoliated graphite/polystyrene composites have been made by similar processing methods. Recently, a commercially viable process was developed for polystyrene in which montmorillonite intercalated with octadecyl trimethyl ammonium chloride was melt-mixed with a styrene methylvinyloxazoline copolymer. This process resulted in complete exfoliation, which could not be achieved with pure polystyrene. The hypothesis is that the hybridization is due to strong hydrogen bonding between the oxazoline groups and oxygen groups in the silicate clays.

2.3.2.4 Epoxy and Polyurethane Matrices

Epoxy is a widely used thermoset, with applications ranging from household glues to high-performance composites. To improve performance, increasing the Tg of epoxy and improving its properties above the Tg are desirable. Adding clays and layered silicic acids to epoxy can greatly improve its mechanical performance, particularly at temperatures above Tg. The processing has been studied in detail. In the smectic clay/epoxy composites, the length of the intercalated organic amine determines the ease of exfoliation, and only clays with primary and secondary onium ions form exfoliated nanocomposites. After intercalation of the organic amines, the epoxy resin or a combination of resin and curing agent can be intercalated into the smectic clays or layered silicic acids. If enough resin and curing agent are intercalated and the curing process is controlled, exfoliated nanocomposites result.

2.3.3 Nanoparticle/Polymer Composite Processing

There are three general ways of dispersing nanofillers in polymers. The first is direct mixing of the polymer and the nanoparticles either as discrete phases or in solution. The second is in-situ polymerization in the presence of the nanoparticles, and the third is both in-situ formation of the nanoparticles and in-situ polymerization. The latter can result in composites called hybrid nanocomposites because of the intimate mixing of the two phases.

2.3.3.1 Direct Mixing

Direct mixing takes advantage of well established polymer processing techniques. For example, polypropylene and nanoscale silica have been mixed successfully in a two-roll mill, but samples with more than 20 wt. % filler could not

be drawn. This is typical and is a limitation of this kind of processing method. Nanoscale silica/PP composites have been processed in a twin-screw extruder, but the dispersion was successful only after modification of the silica interface to make it compatible with the matrix. A Brabender high-shear mixer has been successfully used to mix nanoscale alumina with PET, LDPE. Thermal spraying has also been successful in processing nanoparticle-filled Nylon. When these traditional melt-mixing or elastomeric mixing methods are feasible, they are the fastest method for introducing new products ton market, because the composites can be produced by traditional methods. This has been successful in many cases, but for some polymers, the viscosity increases rapidly with the addition of significant volume fractions of nanofiller, which in turn can limit the viability of this processing method. In addition to viscosity effects, nanoparticles can either enhance or inhibit polymer degradation. One method for measuring degradation is to place the polymer in a highshear mixer and measure the torque as a function of time and temperature. As the material crosslinks, the torque begins to increase (at a constant speed), and when chain scission begins, the torque decreases. This leads to a peak in the torque, whose position is often used as a measure of the degradation time. A recent study on ZnO/LDPE composites showed that, for nanoparticle/matrix mixtures, the time at the peak increased by a factor of almost 2; however, micrometer-size particles decreased the degradation time. In other instances, the catalytic nature of the nanoparticles greatly decreases the degradation time. Whether degradation is inhibited or enhanced depends on the particle surface activity and the increased interfacial area (particle size).

2.3.3.2 Solution Mixing

Some of the limitations of melt-mixing can be overcome if both the polymer and the nanoparticles are dissolved or dispersed in solution. This allows modification of the particle surface without drying, which reduces particle agglomeration. The nanoparticle/polymer solution can then be cast into a solid, or the nanoparticle/polymer can be isolated from solution by solvent evaporation or precipitation. Further processing can be done by conventional techniques.

2.3.3.3 In-Situ Polymerization

Another method is in-situ polymerization. Here, nanoscale particles are dispersed in the monomer or monomer solution, and the resulting mixture is polymerized by standard polymerization methods. One fortunate aspect of this method is the potential to graft the polymer onto the particle surface. Many different types of nanocomposites have been processed by in-situ polymerization. A few examples are silica/Nylon6, silica/poly 2-hydroxyethylmethacrylate, alumina/polymethylmethacrylate, titania/PMMA, and $CaCO_3$/PMMA. The key to in-situ polymerization is appropriate dispersion of the filler in the monomer. This often requires modification of the particle surface because, although dispersion is easier in a liquid than in a viscous melt, the settling process is also more rapid.

2.4 LITERATURE REVIEW

Antisari M.V. *et.al*, 2003. used an electric arc discharge performed in liquid environments between pure graphite electrodes. The synthesis of MWCN by arc discharge submerged in deionizer water and liquid nitrogen. Electron microscopy observations of both the reaction products and the surface of the as-synthesized raw material showed the presence of structural degradation of the MWCN, which probably operates after their growth at the cathode. The degradation is tentatively ascribed to a combination of overheating and high current density experienced by the as-synthesized MWNT, which can be caused by the loose structure of the as-deposited material. The damage appeared to be less severe in water environments, probably owing to the better cooling capacity of water relative to liquid nitrogen.

Chang T.E. *et.al*, 2005 analyzed mechanical properties and structure of polypropylene fibers with different concentrations of single-wall carbon nanotubes (SWNTs) and draw down ratios (DDR). Tensile tests show a three times increase in the Young's modulus with addition of only 1 wt% SWNT, and much diminished increase of modulus with further increase in SWNT concentration. Microscopic study of the mechanism of reinforcement by SWNT included Raman spectroscopy and wide-angle X-ray diffraction (WAXD). The results show linear transfer of the applied stress from the polymer matrix to SWNT. Analysis of WAXD data demonstrates formation of a b-crystal phase in polypropylene matrix under the strain.

Cui S. *et.al.*, 2002 used a several methods to prepare carbon nanotubes (CNTs). The atmosphere, under which the arc discharge is made, is one of the

important and key factors affecting the yield and the morphology of CNTs. The cost of MWCNT production can be reduced remarkably hereby, compared to helium or H_2 atmospheres, respectively. The present problem is that the selectivity is not good. However, the selectivity may be improved by changing and optimizing the arc discharge conditions. Another problem is that the source products formed in the plasma during the arc discharge under nitrogen atmosphere may be harmful. This problem may be overcome by passing the tail gas through an absorbing bath.

Lange H. et.al., 2003 used an arc discharge in water between pure and catalyst-doped graphite electrodes. Emission spectroscopy was performed to assess the plasma components (H, O, C and C_2) and temperature values. C_2 radicals were determined quantitatively, between 10^{15} and 10^{16} cm^2 depending on graphite anode composition. The temperature was between 4000 and 6500 K This study has shown that water arc-discharge technology simplifies the traditional He discharge for CNT production no special equipment, vacuum or gas are needed. Further-more, this technique facilitates the collection of products from the water surface, rather than from the whole of the dusty reaction chamber.

Sano N. *et.al*, 2004 used a novel nanocarbon structure, carbon nanohorns (CNHs) particle which includes one Ni-contained carbon nanocapsule (CNC) in its center, is produced by submerged arc in liquid nitrogen using Ni-contained (0.7 mol%) graphite anode. Transmission electron microscopy revealed that each CNHs particle in nearly spherical shape of diameter around 50–100 nm has one Ni nanoparticle of diameter 5–20 nm encapsulated by graphitic shells as CNC Production rate of powders containing CNHs and CNHs–CNC hybrid particles was 0.57 mg s^{-1}.

The concentration of CNHs–CNC hybrid particles among CNHs particles seemed still very low under the present condition, which would be much less than 1%, so that it is necessary to optimize the concentration of doped Ni in anode for high yield of CNHs–CNC hybrid particles.

Sano N. *et.al.*, 2003 used an arc discharge between a graphite cathode and a molybdenum anode filled with microscopic MoS_2 powder submerged in de-ionized water. A statistical study of over 150 polyhedral fullerene-like MoS_2 nano-particles in plan view transmission electron microscopy revealed that the majority consisted of 2–3 layers with diameters of 5–15 nm. The nano-particles are formed by seamless folding of MoS_2 sheets. A model based on the agglomeration of MoS_2 fragments over an extreme temperature gradient around a plasma ball in water is proposed to explain the formation of nano-particles.

Sano N. *et.al.*, 2004 used an arc discharge method to fabricate high-quality nanoparticles including spherical carbon onions and elongated fullerene-like nanoparticles similar to nanotubes in large quantities without the use of vacuum equipment. The nanoparticles are obtained in the form of floating powder on the water. HRTEM and SEM images confirm the presence of spherical carbon onions with diameters ranging from 4 to 36 nm. The specific surface area of the obtained particles is as large as 984.3 m^3/g. The large specific surface area can be attributed to the "surface roughness" induced by the defective nature of the carbon onion shells. To explain the formation mechanism of the carbon onions, a model of arc discharge in water with two quenching zones is proposed (1) the presence of ion current conductive of elongated nanoparticles growth and (2) the absence of ion current for

isotropic growth of carbon onions. They propose that the physical characteristics of the product can be controlled by manipulating voltage of electricity supplied to the electrodes.

Sano N., 2004 used a cost-effective technique lately proposed to fabricate carbon nanomaterials, which does not require vacuum facilities. Currently, it is demanded to examine the effect of liquid components on the products synthesized by this method. In this study, liquid benzene (C_6H_6) was used in the 'arc in liquid' method. As a result, multi-shelled nanoparticles of diameter 10–30 nm were found in the deposits formed between electrodes, in which highly curled graphitic structure seemed majority. Importantly, CNTs are not formed in this condition, which is different from arc in water or liquid nitrogen. As a result, multishelled nanoparticles of diameter 10–30 nm were found in the deposits formed between electrodes, in which highly curled graphitic structure seemed majority. CNTs are not formed in this condition, which is different from arc in water or liquid nitrogen. In addition, it was confirmed that fullerene was not produced by the present condition.

Zhu H.W. *et.al*, 2002 used a simplified arc discharge apparatus for growing carbon nanotubes, required only water (solution) in a glass container with no need for vacuum, water-cooled chamber. Carbon nanotubes with highest purity (20%) and highest yield (7 mg/min) were obtained when using salt solution as the medium. The results show that high-quality MWNTs can be effectively prepared in water-arcingprocess Based on this idea; a modified water-protected arc discharge technique has been developed by us recently for efficient and continuous production of CNTs with a high production rate and yield.